

More than Steric Effects: Unlocking the Coordination Chemistry of Barium Pyrazolates

Anna Y. O'Brien,^[a] Julia Hitzbleck,^[a,b] Ana Torvisco,^[a] Glen B. Deacon,^[b] and Karin Ruhlandt-Senge*^[a,b]

Keywords: Pyrazolates / Barium / N ligands / Coordination modes / Structure elucidation / CVD precursors / Synthetic methods

To further our understanding of the coordination chemistry of the heavy alkaline earth metals, we here report on a family of barium pyrazolates bearing various substitution patterns that illustrate the delicate balance between ligand bulk, donor size, stoichiometry, and hapticity, while emphasizing the importance of secondary interactions including π -bonding, agostic interactions, and hydrogen bonding to stabilize these heavy-metal complexes. The dimeric compounds $[\{\text{Ba}(\text{Me}_2\text{-}$

$\text{pz})_2(\text{pmdta})_2\}$ (1), $[\{\text{Ba}(\text{Phpz})_2(\text{pmdta})_2\}]_2$ (2), $[\{\text{Ba}(\text{tBupz})_2(\text{pmdta})_2\}]_2$ (3), $[\{\text{Ba}(\text{MePhpz})_2(\text{tmeda})_2\}]_2$ (5), $[\{\text{Ba}(\text{Ph}_2\text{pz})_2(\text{tmeda})_2\} \cdot \text{TMEDA}$ (6), the polymer $[\{\text{Ba}(\text{tBupz})_2(\text{NH}_3)_2\}]_n$ (4), and the monomer $[\text{Ba}(\text{Ph}_2\text{pz})_2(\text{tmeda})_2] \cdot \text{TMEDA}$ (7), were prepared using a variety of synthetic methods and were characterized spectroscopically and structurally.

(© Wiley-VCH Verlag GmbH & Co. KGaA, 69451 Weinheim, Germany, 2008)

Introduction

In the quest for volatile, thermally robust CVD precursors of the heavy alkaline earth metals, metal-organic barium reagents remain a priority.^[1–4] For large metals such as barium, the prediction of the coordination chemistry is difficult due to weak metal–ligand and metal–donor interactions and tendency towards aggregation. Thus, a better understanding and control of factors governing the steric saturation of the metal center is critically needed. With many competing factors, such as solvation vs. ligation and possible secondary interactions, systematic studies comparing such influences are beneficial.

Solvation by a sterically demanding neutral donor is common practice for reducing aggregation in metal-organic compounds of larger metals, such as barium. With a range of possible substitution patterns, and thus control over steric demand, as well as solubility, the pyrazolate ligand system has been of interest as an alternative to oxygen-containing β -diketonates. In this paper, we report a systematic study of barium pyrazolate compounds with varied substitution patterns (see Figure 1) in the presence of various neutral donors.

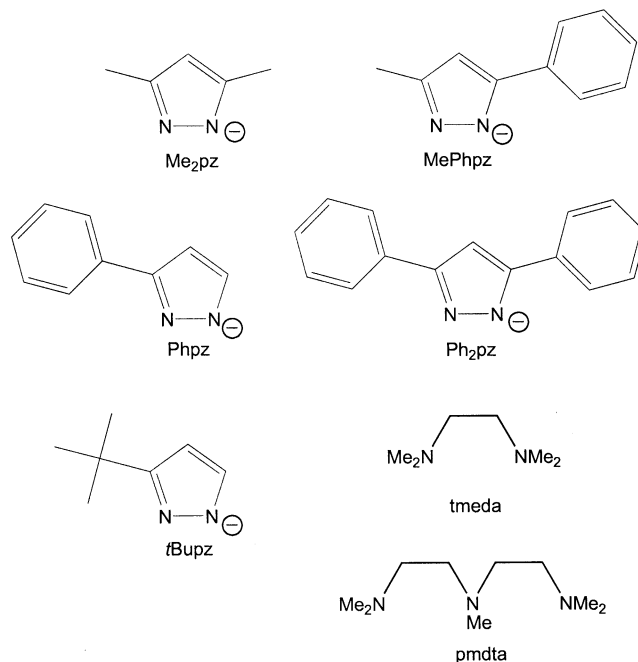


Figure 1. Pyrazolate substitution patterns and neutral donors with abbreviations.

Through the course of this and previous work, it has become apparent that secondary interactions play an equally important role as steric saturation in heavy alkaline earth metal pyrazolates.^[4] These secondary interactions include π -bonding, hydrogen bonding, and agostic interactions, as observed in the crystal structures of a number of pyrazolates such as $[\text{Ba}_6(\text{tBu}_2\text{pz})_{12}]$,^[4c] $[\text{Sr}(\text{Me}_2\text{pz})_2(\text{Me}_2\text{-}$

[a] Department of Chemistry, 1-014 Center for Science and Technology, Syracuse University, Syracuse, NY 13244-4100, USA
Fax: +1-315-443-4070
E-mail: kruhlandt@syr.edu

[b] School of Chemistry, Monash University, Clayton, Victoria 3168, Australia
Fax: +61-3-9905-4597
E-mail: Glen.Deacon@sci.monash.edu.au

Supporting information for this article is available on the WWW under <http://www.eurjic.org> or from the author.

pzH₄],^[4d] and [$\{\text{Sr}(\text{tBu}_2\text{pz})_2(\text{thf})_2\}_2$],^[4b] respectively. Others have reported the significance of secondary interactions of the related barium tetrazolate compounds, Ba[CN₄(NMe₂)₂]₂ (18-crown-6) and Ba[CN₄(NiPr₂)₂](18-crown-6),^[5] where weak C–H⋯N interactions between donors and tetrazolate ligands are believed to influence the tetrazolate coordination modes.

These data also show that the understanding of the coordination chemistry of the heavy alkaline earth metals lags far behind that for magnesium, prompting us to initiate a detailed study into the coordination chemistry of barium pyrazolates. By focusing on one metal, we can better evaluate the effects of the steric demand of the pyrazolate ligand and the nature and stoichiometry of the donor, as well as the influence of secondary interactions. In this report, we discuss these effects in a comprehensive and systematic fashion by analyzing a family of new barium pyrazolate compounds: five dimeric complexes [$\{\text{Ba}(\text{Me}_2\text{pz})_2(\text{pmdta})\}_2$] (**1**), [$\{\text{Ba}(\text{Phpz})_2(\text{pmdta})\}_2$] (**2**), [$\{\text{Ba}(\text{tBupz})_2(\text{pmdta})\}_2$] (**3**), [$\{\text{Ba}(\text{MePhpz})_2(\text{tmeda})\}_2$] (**5**), and [$\{\text{Ba}(\text{Ph}_2\text{pz})_2(\text{tmeda})\}_2 \cdot \text{TMEDA}$] (**6**), one monomer [Ba(Ph₂pz)₂(tmeda)₂] \cdot TMEDA (**7**), and one polymer [$\{\text{Ba}(\text{tBupz})_2(\text{NH}_3)_2\}_n$] (**4**), along with previously reported compounds.

Results and Discussion

(i) Preparation of Barium Pyrazolates

Transamination (method A) and salt metathesis (method D) have been well established, but require the preparation of air-sensitive starting materials.^[4d,6] We here show direct metallation either at elevated temperatures (method C) or in anhydrous liquid ammonia (method B) to be facile, inexpensive, one-step routes. Workup of the reaction products is simple due to the gaseous hydrogen byproduct.^[4d] More-

over, direct metallation at elevated temperatures is done in the absence of organic solvents or transmetallating agents (i.e. HgR₂) (Scheme 1).

Method	Synthetic route	Product
A	$[\text{M}(\text{N}(\text{SiMe}_3)_2)_2(\text{thf})_2] + 2 \text{pzH} \xrightarrow[\text{Solvent}]{n \text{ Donor}}$	$\text{Mpz}_2(\text{Donor})_n + 2 \text{HN}(\text{SiMe}_3)_2$
B	$\text{M} + 2 \text{pzH} \xrightarrow[\text{Solvent, NH}_3(l)]{n \text{ Donor}}$	$\text{Mpz}_2(\text{Donor})_n + \text{H}_2$
C	$\text{M} + 2 \text{pzH} \xrightarrow[2) \text{ Solvent, Donor}]{1) 200-300 \text{ }^\circ\text{C}}$	$\text{Mpz}_2(\text{Donor})_n + \text{H}_2$
D	$\text{MX}_2 + 2 \text{Kpz} \xrightarrow[\text{Solvent}]{n \text{ Donor}}$	$\text{Mpz}_2(\text{Donor})_n + 2 \text{KX}$

M = Ca, Sr, Ba; Donor = TMEDA, PMDTA, NH₃; X = Br, I

Scheme 1. Synthetic routes.

The dimeric compounds [$\{\text{Ba}(\text{Me}_2\text{pz})_2(\text{pmdta})\}_2$] (**1**), [$\{\text{Ba}(\text{Phpz})_2(\text{pmdta})\}_2$] (**2**), and [$\{\text{Ba}(\text{tBupz})_2(\text{pmdta})\}_2$] (**3**) (Figures 2, 3, and 4) were synthesized according to method B, introducing stoichiometric amounts of PMDTA to the initial reaction mixtures. In addition, **1** was also obtained by method A with a stoichiometric amount of PMDTA, and **3** was also obtained by method C after extraction with a hexane/PMDTA solution.

In the absence of a secondary donor, synthesis by method B resulted in the formation of a polymeric barium complex [$\{\text{Ba}(\text{tBupz})_2(\text{NH}_3)_2\}_n$] (**4**) (Figure 5), with ammonia as the coordinated neutral donor. The dimeric compounds [$\{\text{Ba}(\text{MePhpz})_2(\text{tmeda})\}_2$] (**5**) and [$\{\text{Ba}(\text{Ph}_2\text{pz})_2(\text{tmeda})\}_2 \cdot \text{TMEDA}$] (**6**) (Figures 6 and 7) were also prepared by method B through the addition of stoichiometric amounts of TMEDA to the initial reaction mixtures. Use of TMEDA in excess quantities resulted in the formation of the monomeric [Ba(Ph₂pz)₂(tmeda)₂] \cdot TMEDA, **7** (Figure 8).

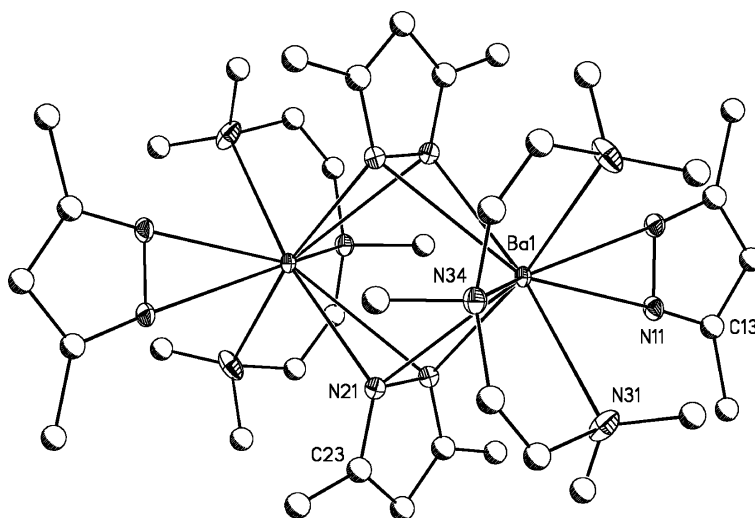


Figure 2. [$\{\text{Ba}(\text{Me}_2\text{pz})_2(\text{pmdta})\}_2$] (**1**) with anisotropic displacement parameters depicting 50% probability. Hydrogen atoms have been removed for clarity.

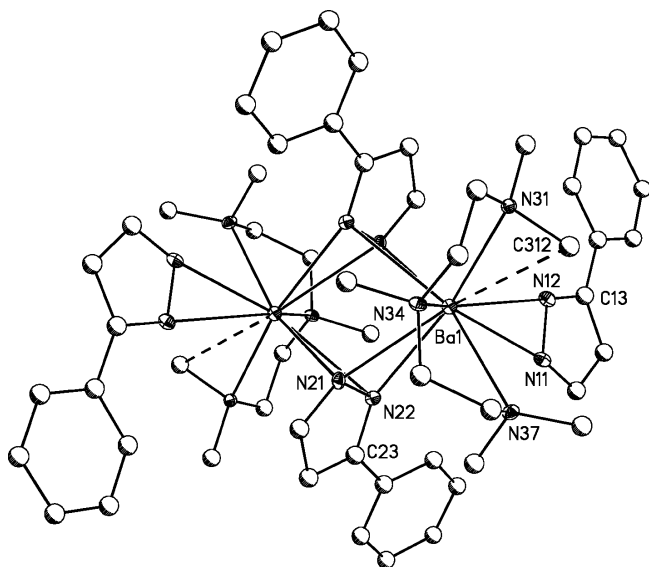


Figure 3. $[\{\text{Ba}(\text{Phpz})_2(\text{pmdta})\}_2]$ (2) with anisotropic displacement parameters depicting 50% probability. Hydrogen atoms have been removed for clarity.

Attempts to reduce the nuclearity through the use of excess PMDTA during the synthetic procedures for 1–3 resulted in intractable product mixtures, in line with the re-

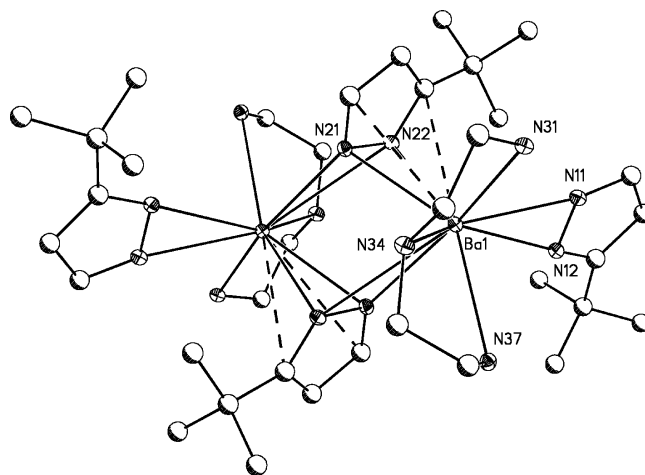


Figure 4. $[\{\text{Ba}(t\text{Bupz})_2(\text{pmdta})\}_2]$ (3) with anisotropic displacement parameters depicting 50% probability. Hydrogen atoms and PMDTA methyl groups have been removed for clarity.

ported 1:1 stoichiometry of donor/metal which was employed for the formation of $[\text{Ba}(t\text{Bu}_2\text{pz})_2(\text{tetraglyme})]$ and $[\text{Ba}(t\text{Bu}_2\text{pz})_2(\text{triglyme})]$ by Winter et al.^[3a] Conversely, our group has reported a group of heavy alkaline earth metal pyrazolates which were reduced in nuclearity from the

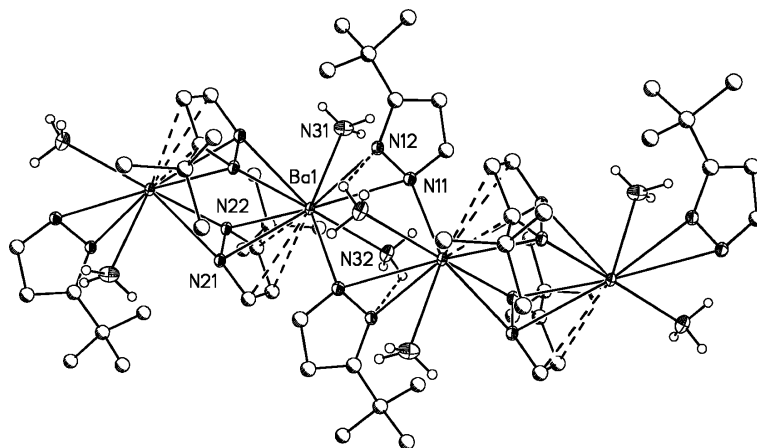


Figure 5. Fragment of $[\{\text{Ba}(t\text{Bupz})_2(\text{NH}_3)_2\}_n]$ (4) with anisotropic displacement parameters depicting 50% probability. Hydrogen atoms have been removed from pyrazolate ligands for clarity.

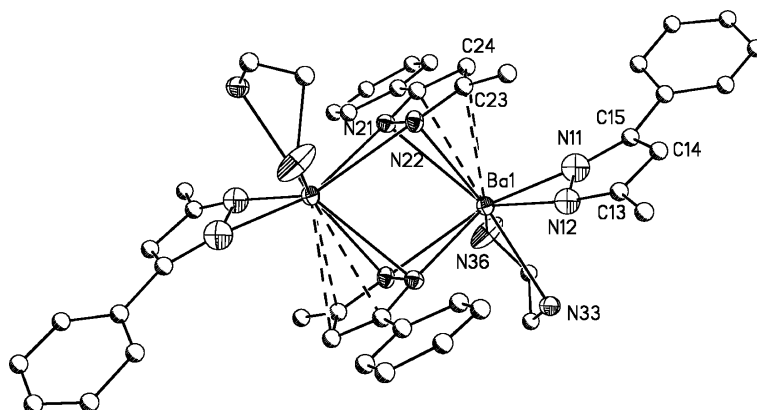


Figure 6. Molecular representation of $[\{\text{Ba}(\text{MePhpz})_2(\text{tmeda})\}_2]$ (5). Disordered components have been removed for clarity.

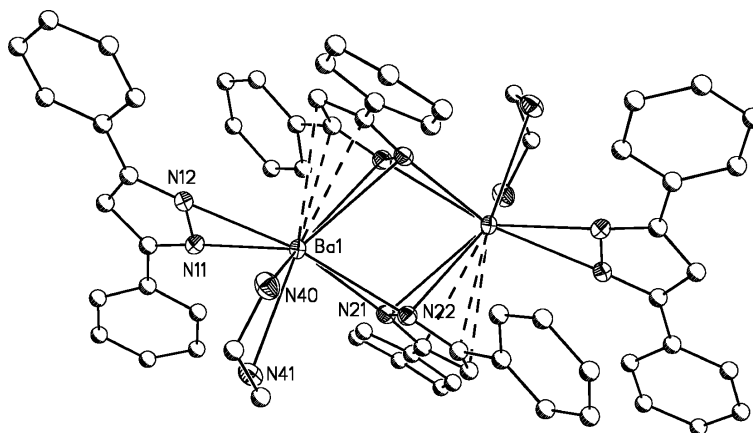


Figure 7. $[\{\text{Ba}(\text{Ph}_2\text{pz})_2(\text{tmeda})\}_2]\cdot\text{TMEDA}$ (**6**) with anisotropic displacement parameters depicting 50% probability. The solvent of crystallization TMEDA, hydrogen atoms and TMEDA methyl groups have been removed for clarity.

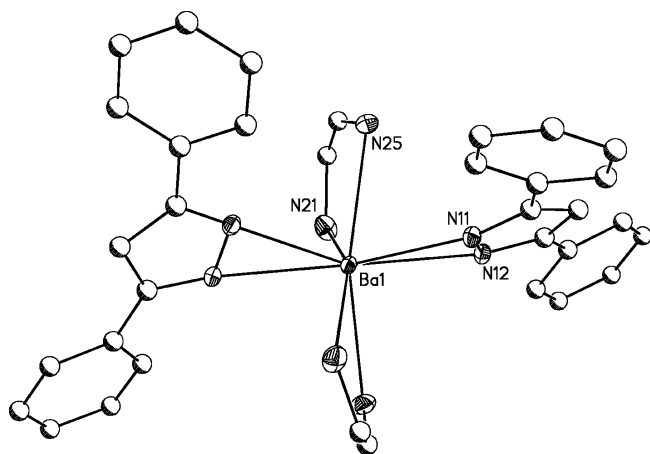


Figure 8. $[\text{Ba}(\text{Ph}_2\text{pz})_2(\text{tmeda})_2]\cdot\text{TMEDA}$ (**7**) with anisotropic displacement parameters depicting 50% probability. The solvent of crystallization TMEDA, hydrogen atoms, TMEDA methyl groups, and the minor disordered components have been removed for clarity.

oligomeric $[\{\text{M}(\text{tBu}_2\text{pz})_2\}_n]$ ($\text{M} = \text{Ca}$, $n = 3$; $\text{M} = \text{Sr}$, $n = 4$; $\text{M} = \text{Ba}$, $n = 6$) to the dimeric $[\{\text{M}(\text{tBu}_2\text{pz})_2(\text{thf})_x\}_2]$ ($x = 1$, $\text{M} = \text{Ca}$, Sr ; $x = 2$, $\text{M} = \text{Ba}$) by dissolving the oligomeric compounds in tetrahydrofuran (thf).^[4b,4c] Thus, the use of reaction stoichiometry to control the product nuclearity may be limited by the ease with which the product can be isolated from the excess of neutral donor.

(ii) Structure Descriptions

Low-temperature single-crystal X-ray structure determinations have been carried out for the compounds **1–7**. Severe disorder in **5** prevented a quality-data refinement, but we present an illustration of **5** (Figure 6) to show the connectivity. A structural description of compounds **1–4** and **6–7** follows. Descriptive data are given in Table 1, while additional bond lengths and angles are given in the Supporting Information.

In most cases, the geometry of the barium atom can be described by approximating σ - η^2 -bonding of the pyrazolate ligands as connected through the center of the N–N bond [(cen)_{N–N}, see Figure 9a], on the basis of the narrow bite angle (N–Ba–N), and the symmetry of the Ba–N bond lengths ($\Delta_{\text{Ba–N}}$). For terminal σ - η^2 -bonded pyrazolates, this approximation is also justified by the near co-planarity of the terminal pyrazolate ring with the Ba–N–N plane. For bridging pyrazolates which include π -bonded ligands (η^{3-5}) a similar approximation can be made, based on the distance from the barium atom to the centroid of the pyrazolate ring [(cen)_{pz}].

The extent of the π -character of a pyrazolate–metal interaction is discussed in terms of Ba–C distances as well as the following geometric details: the angle between the plane of a pyrazolate and a vector connecting the centroid of the pyrazolate ring to the metal atom (Ba/pz angle) gives an indication of π -interactions; the optimum orientation for π -interactions is a 90° Ba/pz angle (see Figure 9b). Additionally, for bridging pyrazolates, the angle between the barium–barium axis and the plane of the bridging pyrazolate (tilt angle) gives an indication of the extent of the inclination and π -interactions. For example, a pyrazolate plane perpendicular to the barium–barium axis (tilt angle 90°) indicates perfectly symmetrical μ - η^2 : η^2 -bridging (see Figure 9c).

The complexes $[\{\text{Ba}(\text{Me}_2\text{pz})_2(\text{pmdta})\}_2]$ (**1**), $[\{\text{Ba}(\text{Phpz})_2(\text{pmdta})\}_2]$ (**2**), and $[\{\text{Ba}(\text{tBupz})_2(\text{pmdta})\}_2]$ (**3**) are all centrosymmetric dimers, with two barium atoms bridged by two pyrazolates. Each barium atom is further coordinated by a terminal η^2 -pyrazolate and a tridentate PMDTA donor. This results in a formal coordination number of 9; however, if the pyrazolate binding is approximated as monodentate, as described above, each barium atom can be assigned a distorted octahedral environment (see Table 1).

A coordinatively unsaturated area on the face of the barium atom between the bridging and terminal pyrazolates [(cen)_{N–N}–Ba–(cen)_{N–N} 114.96° (**1**), 110.38° (**2**), (cen)_{N–N}–Ba–(cen)_{pz} 105.5° (**3**)] arises from the restricted bite of the

Table 1. Structural description data for **1–4**, **6–7**.

	1	2	3	4	6	7
Bridging mode	$\mu\text{-}\eta^2\text{:}\eta^2$	$\mu\text{-}\eta^2\text{:}\eta^2$	$\mu\text{-}\eta^4\text{:}\eta^2$	$\mu\text{-}\eta^5\text{:}\eta^2$ and $\mu\text{-}\eta^2\text{:}\eta^1$	$\mu\text{-}\eta^5\text{:}\eta^2$	NA
CN of Ba	9	10	11	12	11	8
Axial	η^2 -bound	η^2 -bound	η^4 -bound	η^5 -bound	η^5 -bound	η^2 -bound
N–Ba–N [°]	27.2(1)	26.77(8)	27.24(6)	26.71(6)	26.52(10)	29.10(4)
Ba–(cen) _{N–N} [Å]	2.846	2.904	NA	NA	NA	2.639
Ba–(cen) _{pz} [Å]	NA	NA	3.048	2.982	2.890	NA
Ba–N [Å]	2.807(3)	2.935(3)	2.928(2)	2.965(2)	2.910(4)	2.684(1)
	3.048(3)	2.966(3)	2.955(2)	3.048(2)	3.053(4)	2.768(2)
$\Delta_{\text{Ba–N}}$ [Å]	0.214	0.099	0.027	0.083	0.143	0.084
Ba–C [Å]	NA	NA	3.346(3)	3.202(3)- 3.396(2)	3.058(5)- 3.281(5)	NA
Ba/pz angle [°]	NA	61.4	69.5	77.5	81.4	NA
Tilt angle [°]	90.0	64.6	58.3	47.3	43.5	NA
Axial	N _{PMDTA}	N _{PMDTA}	N _{PMDTA}	η^2 -bound	N _{TMEDA}	η^2 -bound
N–Ba–N [°]	NA	NA	NA	27.47(6)	NA	29.10(4)
Ba–(cen) _{N–N} [Å]	NA	NA	NA	2.831	NA	2.639
Ba–N [Å]	2.965(4)	3.070(3)	3.039(2)	2.942(2) 2.886(2)	2.890(4)	2.684(1) 2.768(2)
$\Delta_{\text{Ba–N}}$ [Å]	NA	NA	NA	0.056	NA	0.084
Equatorial	N _{PMDTA}	N _{PMDTA}	N _{PMDTA}	N _{NH3}	N _{TMEDA}	N _{TMEDA}
Ba–N [Å]	2.933(5)	2.966(3)	2.957(2)	2.897(3)	2.880(4)	2.906(2)
Equatorial	N _{PMDTA}	N _{PMDTA}	N _{PMDTA}	N _{NH3}	NA	N _{TMEDA}
Ba–N [Å]	2.965(4)	2.910(3)	2.983(2)	2.928(3)	NA	2.995(2)
Equatorial	η^2 -bound	η^2 -bound	η^2 -bound	η^2 -bound	η^2 -bound	N _{TMEDA}
N–Ba–N [°]	27.2(1)	28.54(8)	23.84(6)	28.76(7)	28.62(11)	NA
Ba–(cen) _{N–N} [Å]	2.846	2.722	3.014	2.712	2.695	NA
Ba–N [Å]	2.807(3)	2.801(3)	2.799(2)	2.775(2)	2.775(4)	2.906(2)
	3.048(3)	2.817(3)	3.360(2)	2.825(2)	2.788(4)	
$\Delta_{\text{Ba–N}}$ [Å]	0.214	0.016	0.561	0.050	0.013	NA
Equatorial	η^2 -bound	η^2 -bound	η^2 -bound	η^1 -bound	η^2 -bound	N _{TMEDA}
N–Ba–N [°]	29.7(1)	29.02(8)	29.44(6)	NA	29.26(11)	NA
Ba–(cen) _{N–N} [Å]	2.609	2.722	2.626	NA	2.613	NA
Ba–N [Å]	2.699(3)	2.712(3)	2.711(2)	2.842(2)	2.678(4)	2.995(2)
		2.776(3)	2.720(2)		2.723(4)	
$\Delta_{\text{Ba–N}}$ [Å]	0.00	0.064	0.09	NA	0.045	NA
Deviation from planarity [°]	1.4	10.2	10.2	NA	1.5	NA
Tilt angle [°]	NA	NA	NA	84.4	NA	NA

equatorial PMDTA nitrogen atoms [N–Ba–N 61.96° (**1**), 59.70° (**2**), 61.7° (**3**)]. Each dimer “fills” this exposed area in a unique way. In **1**, the bridging pyrazolates bind asymmetrically ($\Delta_{\text{M–N}}$ 0.241 Å). Steric repulsion between the PMDTA and the methyl substituents of the pyrazolate results in a longer Ba–N distance on the pyrazolate nitrogen atom closest to the PMDTA [Ba(1)–N(21) 3.048(3) Å], creating an unsaturated area that causes the pyrazolate to twist. This leads to a shorter Ba–N distance [Ba(1)–N(21) #3 2.807 Å] and a Ba–C bond length [Ba(1)–C(23)#3 3.829 Å] just within the sum (3.90–3.97 Å) of the van der Waals radius of a barium atom [2.17(CN = 8) to 2.24 (CN = 12) Å] and the van der Waals radius of a π -bonded carbon atom of a phenyl ring (1.73 Å).^[7] The Ba...C separation lies outside of established values for π -bonding between a substituted pyrazolate ring and a barium atom

(3.056–3.39 Å),^[3b,4,8,9] and beyond the weakly bonding Ba–C distance [3.499(2) Å] found in [$\{\text{Ba}(t\text{Bu}_2\text{pz})_2(\text{thf})_2\}_2$].^[4b] Accordingly, the bridging pyrazolates are considered to have $\mu\text{-}\eta^2\text{:}\eta^2$ -bonding interactions, with a tilt angle of 90°.

In compound **2**, this void is filled by an agostic interaction from a methyl group of the PMDTA [Ba–C(312) 3.277(4) Å], in contrast to the twisting of the bridging pyrazolate observed in **1**. The coordination of the bridging pyrazolates in **2** is described as $\mu\text{-}\eta^2\text{:}\eta^2$ because the Ba–C distances (3.508–3.952 Å) lie outside of the values reported for π -bonded pyrazolates (vide supra). However, the tilt angle (64.6°) deviates significantly from the ideal 90° and other known values for $\mu\text{-}\eta^2\text{:}\eta^2$ -bonding {90.0° (**1**) and 87.8(9)° [Ba₆(*t*Bu₂pz)₁₂]^[4c]}, consistent with weak π -interactions. Yet, the tilt angle in **2** is not small enough to imply significant π -bonding when compared to values reported for μ -

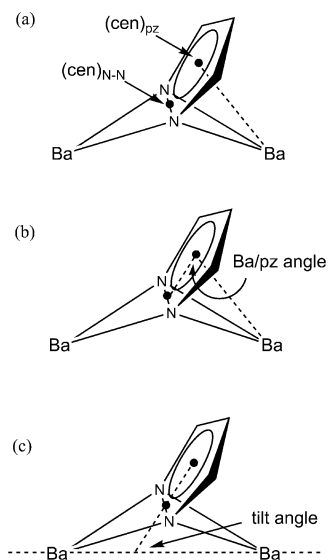


Figure 9. Angles used in structural analysis (a) location of centroids, (b) Ba–cen/pz angle (c) tilt angle.

$\eta^5:\eta^2$ -bridging pyrazolates in [(thf)₆Ba₆(Me₂pz)₈{(OSiMe₂)₂O}]₂ (45.8°, 54.1°),^[9] [Ba₆(*t*Bu₂pz)₁₂] (45.6°, 47.2°)^[4c] and the $\mu\text{-}\eta^4:\eta^2$ -bridging pyrazolates in [{Ba(*t*Bu₂pz)₂(thf)₂}]₂ (48.7°)^[4b] and [Ba₆(*t*Bu₂pz)₁₂] (44.8°, 44.7°).^[4c] Thus, the bridging is considered to be $\mu\text{-}\eta^2:\eta^2$.

The vacancy in the coordination sphere in **3** is filled by donation of π -pyrazolate electrons in an η^4 -interaction, because the Ba–C distances for the 3,5-positions [C(23) 3.396(2), C(25) 3.346(3) Å] fall within established π -bonding values (vide supra), while the carbon atom in the 4-position [Ba(1)–C(24) 3.640 Å] does not (vide supra).

The polymeric barium complex, [{Ba(*t*Bupz)₂(NH₃)₂}]_n (**4**), has ten-coordinate barium atoms, each bridged by two $\mu\text{-}\eta^5:\eta^2$ - and two $\mu\text{-}\eta^2:\eta^1$ -pyrazolates, in addition to having two terminal neutral ammonia molecules.

The η^5 -bonding mode is justified by the Ba–C distances [C(23) 3.335(3), C(25) 3.202(3) Å] falling within the reported values for barium–pyrazolate π -bonding (vide supra). The third Ba–C distance [C(24) 3.439(3) Å] lies just outside this range, but it is nonetheless shorter than one reported value that is considered a weak π -interaction (vide supra). Accordingly, this interaction is considered to be η^5 -bonding.

The unusual $\mu\text{-}\eta^2:\eta^1$ -bridging mode in **4** is the result of hydrogen bonding between a hydrogen atom of the ammonia donor and the η^1 -bound nitrogen atom [N(32)–H(32B)⋯N(12)#2: N(32)–H(32B) 0.95(4) Å, H(32B)⋯N(12)#2 2.46(4) Å]. Examples of unassisted $\mu\text{-}\eta^2:\eta^1$ -bridging include [Sc₂(Ph₂pz)₆],^[10a] [Li(Ph₂pz)(OEt₂)₂],^[10b] and [Li(*t*Bu₂pz)(*t*Bu₂pzH)₂].^[10c]

The (TMEDA)barium complex [{Ba(MePhpz)₂(tmeda)}₂] (**5**) shows a similar geometrical arrangement to **1–4**, but more pronounced pyrazolate tilting resulting in a $\mu\text{-}\eta^2:\eta^5$ -pyrazolate bridging mode. Due to significant disorder, we present only this general structural trend. Except for slight variations in the inclination of the bridging pyr-

azolates, compound **5** is isostructural with the lighter alkaline earth and rare-earth congeners, [{M(MePhpz)₂(tmeda)}₂] (M = Ca, Yb, Sr, Eu).^[8b]

[{Ba(Ph₂pz)₂(tmeda)}₂]·TMEDA (**6**) crystallizes as a dimer similar to **1–3**, **5** and [{Ba(*t*Pr₂pz)₂(py)₃}]₂.^[4a] Again, approximating the η^2 - and η^5 -coordination of the bridging pyrazolates as monodentate, **6** exhibits a distorted trigonal-bipyramidal metal coordination environment (see Table 1). $\eta^5:\eta^2$ -bound, based on the close Ba–C contacts [3.058(5)–3.281(5) Å] which lie well within the accepted range for Ba–C bonding, the small tilt angle (43.5°), and nearly perpendicular Ba/pz angle (81.4°).

In the monomeric (TMEDA)barium compound [Ba(Ph₂pz)₂(tmeda)₂]·TMEDA **7**, the metal atom is located on a center of symmetry, as such only one ligand and one TMEDA ligand are symmetry-independent, with pairs of ligands and donors arranged in a *transoid* orientation. The formally eight-coordinate metal center exhibits a severely distorted octahedral geometry when the pyrazolates are approximated as monodentate (see Table 1).

(iii) Structural Discussion

The barium pyrazolate complexes presented here join a growing family of reported heavy alkaline earth and rare earth metal pyrazolate complexes that have been structurally characterized.^[3,4,6,8–10] A comprehensive examination of the structures of these complexes lends insight into the different means by which these large metal ions achieve coordinative saturation. Specifically, we look at the effects of pyrazolate substitution and the neutral donor type, with an emphasis on the role of secondary interactions such as π -bonding, agostic interactions, and hydrogen bonding. A comprehensive list of tilt and Ba/pz angles for the barium pyrazolate compounds that contain bridging pyrazolates is found in Table 2.

Ligand Effects: Pyrazolate Substitution

To compare the effects of the pyrazolate ligand substitution, it is useful to examine complexes that have the same metal and neutral donor type, but vary in the ligand substitution pattern. The only reported example of such a set for the heavy alkaline earth metals includes complexes **1–3** (Entries 2, 5, 7; Table 2). In all three compounds, the metal is barium, and PMDTA is used as a donor, with bite angles restricted by the carbon backbone, resulting in a sterically unsaturated area of the barium atom coordination sphere. However, each of the Ba²⁺ ions in each of the three complexes adopt a different strategy to achieve steric saturation. In **1**, the $\mu\text{-}\eta^2:\eta^2$ -bridging pyrazolate twists due to the presence of a methyl group in the 5-position of the pyrazolate ring. In **2**, because of the lack of a substituent in the 5-position, agostic interactions arising from a PMDTA methyl group fill this area. In compound **3**, π -bonding by the bridging pyrazolate fills the exposed area.

These differences illustrate the delicate balance between stabilization by σ - and π -donation and destabilization originating from the steric repulsion between ligands and do-

Table 2. Tilt angles and Ba/pz angles for selected complexes.

Entry	Formula	Binding mode	Tilt angle [°]	Ba/pz [°]	Ref.
1	[{Ba(<i>t</i> Bupz) ₂ (NH ₃) ₂ } _n] (4)	μ-η ² :η ¹	84.4 ^[a]		
2	[{Ba(Me ₂ pz) ₂ (pmdta)} ₂] (1)	μ-η ² :η ²	90.0		
3	[Ba ₆ (<i>t</i> Bu ₂ pz) ₁₂]	μ-η ² :η ²	87.8		[4c]
4	[(thf) ₆ Ba ₆ (Me ₂ pz) ₈ {(OSiMe ₂) ₂ O} ₂]	μ-η ² :η ²	72.8		[9]
5	[{Ba(Phpz) ₂ (pmdta)} ₂] (2)	μ-η ² :η ²	64.6	61.4	
6	[{Ba(<i>i</i> Pr ₂ pz) ₂ (py) ₃ } ₂]	μ-η ² :η ²	63.4	61.1	[4a]
7	[{Ba(<i>t</i> Bupz) ₂ (pmdta)} ₂] (3)	μ-η ⁴ :η ²	58.3	69.5	
8	[{Ba(<i>t</i> Bu ₂ pz) ₂ (thf) ₂ } ₂]	μ-η ⁴ :η ²	48.7	74.5	[4b]
9	[Ba ₆ (<i>t</i> Bu ₂ pz) ₁₂]	μ-η ⁴ :η ²	44.8, 44.7	86, 87	[4c]
10	[{Ba(<i>t</i> Bupz) ₂ (NH ₃) ₂ } _n] (4)	μ-η ⁵ :η ²	47.3	77.5	
11	[(thf) ₆ Ba ₆ (Me ₂ pz) ₈ {(OSiMe ₂) ₂ O} ₂]	μ-η ⁵ :η ²	45.8, 54.1	70, 78	[9]
12	[Ba ₆ (<i>t</i> Bu ₂ pz) ₁₂]	μ-η ⁵ :η ²	45.6, 47.2	80–84	[4c]
13	[{Ba(Ph ₂ pz) ₂ (tmeda)} ₂] · TMEDA (6)	μ-η ⁵ :η ²	43.5	81.4	

[a] Involves hydrogen bonding to η¹-nitrogen atom.

nors. In **1**, the steric repulsion between the methyl groups of the bridging and terminal pyrazolates prevents subsequent tilting and a significant π-contribution from the bridging ligand. The steric repulsion results from the symmetrical arrangement of the terminal pyrazolate with respect to the PMDTA semi-circular arrangement, dictated by its symmetrical 3,5-dimethyl substitution pattern. The symmetrical arrangement might be quantified by the difference in the two smallest N_{terminal-pz}–Ba–N_{(exo)PMDTA} angles [N(11)–Ba(1)–N(31) 78.35(10)°; symmetry required Δ(N–M–N) 0°]. Therefore, the μ-η²:η²-bridging pyrazolate twists (Δ_{M–N} 0.241 Å), rather than tilts (tilt angle 90°), to fill the sterically unsaturated area of the barium atom.

It is instructive to compare the molecular geometry in **1** with [{Ba(*i*Pr₂pz)₂(py)₃}₂]^[4a] (Entry 6, Table 2) where a similar twisting is seen in the μ-η²:η²-bridging pyrazolate (Δ_{M–N} 0.185, 0.176 Å) due to the steric repulsion between the diisopropyl substituents on the terminal and bridging pyrazolates, an effect possibly enhanced by the increased steric demand of three pyridine donors as compared to one tridentate PMDTA. However, [{Ba(*i*Pr₂pz)₂(py)₃}₂] exhibits a more pronounced tilt (63.4°) than **1**, possibly due to the improved electron-donating ability of the isopropyl than the methyl groups, enhancing the tendency of the bridging pyrazolate in [{Ba(*i*Pr₂pz)₂(py)₃}₂] towards π-bonding.

π-Coordination appears to be favored if asymmetrically substituted pyrazolates are employed, as observed in compounds **2** and **3**. Here, the terminally bound pyrazolates are no longer symmetrical with respect to the PMDTA semi-circular arrangement, but arranged to reduce steric repulsion from their asymmetrically located substituents, 3-phenyl in **2** [N(11)–Ba(1)–N(37) 73.37(9)°, N(12)–Ba(1)–N(31) 90.63(9)°; Δ(N–M–N) 17.26°], and 3-*tert*-butyl in **3** [N(11)–Ba(1)–N(31) 75.79(6)°, N(12)–Ba(1)–N(37) 86.47(6)°; Δ(N–M–N) 10.68°]. The reduction of steric repulsion between the substituents of the bridging and terminal pyrazolates allows the bridging pyrazolate to tilt towards the metal atom [tilt angle 64.6° (**2**), 58.3° (**3**)].

The cause of stabilization through agostic interactions, rather than π-coordination in **2** is not obvious, but may be related to (i) the weaker electron-donating ability of the phenyl compared to the *tert*-butyl substituent in **3**, or rather

(ii) the steric repulsion between the terminal methyl groups of the PMDTA and the three-dimensional *tert*-butyl groups of the bridging pyrazolate in **3**. This might prevent the proximity required for agostic interactions to occur or simply provide more coverage of the metal atom than the two-dimensional phenyl ring in **2**.

Donor Effects

The effects of different donors on molecular structure can be analyzed by comparing compounds with the same metal atom and pyrazolate ligand, but different donor types. Several sets of such examples are available.

One set of pyrazolates, which illustrate the effect of different donors, comprises: the hexameric [Ba₆(*t*Bu₂pz)₁₂]^[4c] the dimeric [{Ba(*t*Bu₂pz)₂(thf)₂}₂]^[4b] (Entries 3, 9, 12 and 8, respectively; Table 2), and the monomeric [Ba(*t*Bu₂pz)₂(tetraglyme)] and [Ba(*t*Bu₂pz)₂(triglyme)]^[3a] All contain barium and the *t*Bu₂pz ligand. In this series, a reduction in nuclearity along this list can be attributed to the corresponding increase in donor hapticity and size.

A second set of compounds illustrates another effect. The dimeric **3** and polymeric **4** both employ barium and the asymmetrically substituted *t*Bupz ligand (Entries 1, 7, and 10; Table 2). The arrangement of the ligands and donors about the barium atom in **4** is very similar to that observed in **3**, except that the smaller coordinative and steric requirement of two ammonia donors, as compared to the tridentate PMDTA, results in (i) the increased π-bonding from η⁴ to η⁵, (ii) the conversion of the terminal η²-pyrazolate in **3** to a bridging μ-η²:η¹-arrangement in **4**, and (iii) stabilization through hydrogen bonding of an ammonia hydrogen atom to the uncoordinated nitrogen atom of the η¹-bound pyrazolate.

The ability of the neutral donor to engage in hydrogen bonding usually affects the resulting structure. Other examples of such hydrogen bonding are found in the monomeric [M(Me₂pz)₂(Me₂pzH)₄] (M = Ca, Sr)^[4d] [Mg(*t*Bu₂pz)₂(*t*Bu₂pzH)₂]^[11] and [Nd(η²-Me₂pz)₂(η¹-Me₂pz)(Me₂pzH)-py]^[10a] and the dimeric [{M(*i*Pr₂pz)₂(*i*Pr₂pzH)₂}₂] (M = Mg, Ca, Eu)^[4a] In these complexes, as in **4**, a nitrogen-bound hydrogen atom on the neutral donor (Me₂pzH, *t*Bu₂pzH, or *i*Pr₂pzH vs. NH₃) is donated to a nitrogen

atom of the pyrazolate ring. This hydrogen-bonded embrace reduces pyrazolate hapticity (from η^2 to η^1 in the monomeric compounds^[4d,10a,11] and $[\{Mg(iPr_2pz)_2(iPr_2pzH)_2\}_2]$,^[4a] from $\mu-\eta^2:\eta^2$ to $\mu-\eta^2:\eta^1$ in $[\{Ca(iPr_2pz)_2(iPr_2pzH)_2\}_2]$ ^[4a] and **4**, and from $\mu-\eta^5:\eta^2$ to $\mu-\eta^5:\eta^1$ in $[\{Eu(iPr_2pz)_2(iPr_2pzH)_2\}_2]$).^[4a]

A third set of compounds, **2**, **5**, and **6** (Entries 5, 13; Table 2), vary in both ligand substitution and donor type, but nicely illustrate the tendency towards π -bonding and/or aggregation, upon reduction of the size and/or hapticity of the neutral donor. The reduced coordination number and steric requirements of the bidentate TMEDA in compounds **5** and **6**, as compared to the tridentate PMDTA in **2**, allow for $\mu-\eta^5:\eta^2$ -bridging in **5** and **6** despite the increased steric demand of the ligands by means of an additional phenyl or methyl substituent. Similarly, coordination of only two thf donors in $[\{Ba(tBu_2pz)_2(thf)_2\}_2]$ ^[4b] (Entry 8, Table 2) compared to three pyridine donors in $[\{Ba(iPr_2pz)_2(py)_3\}_2]$ ^[4a] (Entry 6, Table 2) allows for $\mu-\eta^4:\eta^2$ -bridging in the former. Since pyridine and thf have the same steric coordination number values, these dimers vividly illustrate the effect of reduction in bulk from *t*Bu₂pz to *i*Pr₂pz. In the extreme case of the donor-free dimer of trinuclear units $[Ba_6-(tBu_2pz)_{12}]$,^[4c] the dominant π -bonding of the bridging pyrazolates allows the formation of a highly unusual linear arrangement.

Agostic interactions provide an alternative for achieving steric saturation when the metal atom is too small to allow further donor coordination. For example, close M–H contacts were observed in the dimeric compounds $[\{M(tBu_2pz)_2(thf)_2\}_2]$ (M = Sr, Eu) between the metal atom and a *tert*-butyl group of a bridging pyrazolate as well as between the metal atom and a hydrogen atom on an α -position in a thf molecule. Upon increasing the metal size to Ba, the dimeric $[\{Ba(tBu_2pz)_2(thf)_2\}_2]$ was isolated in which agostic interactions were not needed due to the presence of a second thf donor.^[4b]

(iv) Solution Behavior

¹H NMR spectra of the dimeric compounds **1–3**, **5**, and **6** collected at room temperature do not distinguish between terminal and bridging pyrazolates. For example, compound **3** exhibits a single peak observed at $\delta = 1.54$ ppm corresponding to the *t*Bu substituent (see Exp. Sect.), caused by either rapid terminal bridging ligand fluxionality on the NMR time scale or loss of the dimeric structure upon dissolution in the NMR solvent. Similarly, all bridging pyrazolates in **4** displayed the same chemical shifts at room temperature.

As a representative of the dimeric compounds, the solution behavior of **3** was further analyzed by low-temperature ¹H NMR studies in $[D_8]$ toluene. Indeed, upon cooling, splitting of the *t*Bu signal, as well as those of the C4– and C5(pz)–H peaks is observed. From a single peak at 298 K at $\delta = 1.39$ ppm, the *t*Bu signal broadens, and at 238 K begins to split into two broad but distinct peaks. Further

cooling to 194 K affords two cleanly separated peaks. Analogous observations are made for the C4 and C5(pz)–H, peaks with broadening at 233 K, and splitting at 194 K. The dynamic behavior of **3** was analyzed using the Gutowsky–Holm and Eyring equations,^[12] with the free energy of activation ΔG_c^\ddagger for the dynamic exchange of the *t*Bupz ligands in solution estimated to be 11.15 kcal mol^{−1}. Recent variable-temperature ¹H NMR studies in $[D_8]$ toluene of a series of heavy alkaline earth metal pyrazolate dimers $[\{M(tBu_2pz)_2(thf)_x\}_2]$ and homoleptic linear oligomers $[\{M(tBu_2pz)_2\}_n]$ (M = Ca, Sr, Ba),^[4b,4c] also indicated dynamic behavior, but did not allow the computation of ΔG_c^\ddagger due to incomplete peak splitting in both cases. ΔG_c^\ddagger obtained for **3** agrees well with data from previous dynamic studies by Westerhausen et al. focusing on the heavy alkaline earth metal bis[bis(trimethylsilyl)amide] dimers, $\{M[N(SiMe_3)_2]_2\}_2$ (M = Mg, Ca, Sr, Ba).^[13] For the Ca and Sr compounds, ΔG_c^\ddagger was computed to be 17.20 and 12.67 kcal mol^{−1} respectively. The smaller value for the heavier analogue is indicative of the reduced metal–ligand bond strength observed in the heavier analogues.

Conclusions

The analysis of factors influencing the coordination chemistry of the target barium pyrazolates include (i) ligand bulk, (ii) donor size and hapticity, (iii) the capability for secondary interactions (π -bonding, agostic interactions, hydrogen bonding), and (iv) stoichiometry. When steric saturation is not achieved by the steric demand of the ligands and neutral donors, secondary interactions compensate. Their degree and type depend on the pyrazolate substitution pattern, as documented in **1–3**. In the absence of a sterically demanding donor, as seen in **4**, oligomerization takes place. Showing the importance of donor size and hapticity, the comparison of compounds **2** and **6** indicates that the nature of the donor seems to play a more structurally determining role than the steric bulk of the pyrazolate.

Experimental Section

General: All manipulations were carried out under strict exclusion of air and moisture using Schlenk techniques and purified nitrogen or argon. All reagents were stored in a glove box. All solvents were distilled from Na/K alloy and degassed by two freeze-pump-thaw cycles prior to use. The barium metal (ingots, 99.7%, Cerac) was rinsed with hexane before use. Me₂pzH (Lancaster) was dried under vacuum and recrystallized from hexane. PhpzH, *t*BupzH,^[14] *t*Bu₂pzH,^[15] and Ba[N(SiMe₃)₂]₂(thf)₂^[16] were prepared according to literature methods. MePhpzH was synthesized by a modified literature procedure by refluxing the diketone with hydrazine hydrate in ethanol for 24 h.^[17] PMDTA and TMEDA were distilled from CaH₂. Ammonia gas was made anhydrous by being condensed over Na before condensation in a reaction flask. NMR spectroscopic data were obtained with a Bruker Avance spectrometer (300 MHz, 25 °C). The chemical shifts were referenced to the residual solvent signals ($[D_6]$ benzene: $\delta_H = 7.16$ ppm, $\delta_C = 128.38$ ppm; $[D_8]$ thf: $\delta_H = 3.58, 1.73$ ppm; $\delta_C = 67.5, 25.3$ ppm).

Melting points were collected with a MelTemp apparatus in capillaries sealed under nitrogen and are uncalibrated. IR spectra were collected as Nujol mulls using KBr plates with a Perkin–Elmer FT-IR spectrometer. Due to limited quantities, only a representative set of compounds (**2**, **3**) were sent for elemental analysis. However, the correlation between purity of the sample and correctly integrated, clean ^1H NMR spectra for these types of compounds has been demonstrated extensively by our group.^[4] X-ray crystallographic data were collected with a Bruker SMART system, with monochromatic Mo- K_α radiation ($\lambda = 0.71073 \text{ \AA}$), a 3-circle goniometer and APEX CCD detector. Suitable crystals for single-crystal X-ray analysis were removed from a Schlenk tube under a flow of nitrogen gas, immediately covered with viscous hydrocarbon oil (Infineum), and subsequently mounted on a glass fiber with the aid of a microscope.^[18] The mounted crystal remained under a nitrogen flow at low temperature using a custom-built device by H. Hope. For data collection and integration, the Bruker SMART and SAINT software was employed. Empirical adsorption corrections were calculated using the program SADABS.^[19] Solution and refinement with the program SHELXTL-Plus used a total of N unique reflections $\{N_0 [I > 2\sigma(I)] \text{ observed}\}$ in least-squares refinement.^[20] All non-hydrogen atoms were refined anisotropically. Hydrogen atoms were placed in calculated positions. CCDC-649496, -649497, -649498, -649499, -649500, -649501 contain the supplementary crystallographic data for this paper. These data can be obtained free of charge from The Cambridge Crystallographic Data Centre via www.ccdc.cam.ac.uk/data_request/cif. Syntheses of compounds **1**–**7** are as follows (see Scheme 1). Unless otherwise noted, for method B anhydrous ammonia (10 mL) was condensed in a mixture of barium (0.14 g, 1.0 mmol), the appropriate pyrazole, toluene (50 mL) and, if required, neutral donor. Upon complete consumption of the metal, the reaction mixture was warmed slowly to room temperature. If necessary, the solution was passed through a sintered glass frit. The solvent volume was reduced, and the solution was stored at -23°C to yield colorless X-ray quality crystals.

[Ba(Me₂pz)₂(pmdta)]₂ (1). Method B: The general procedure was applied for 3,5-dimethylpyrazole (0.38 g, 4.0 mmol) and PMDTA (0.21 mL, 1.0 mmol). Yield: 0.20 g (40%); m.p. (dec.) over temperature range 70°C (wet) \rightarrow 100 (dry) \rightarrow 170 $^\circ\text{C}$ (wet) suggesting loss of donor. ^1H NMR ($[\text{D}_6]$ benzene): $\delta = 5.76$ [s, 4 H, C4(pz)-H], 2.41 [m, 24 H, N(CH₃)₂], 2.29–2.27 (m, 16 H, CH₂CH₂N), 2.11 [s, 24 H, CH₃(pz)], 1.97 (s, 6 H, NCH₃) ppm. ^{13}C NMR ($[\text{D}_6]$ benzene): $\delta = 144.5$ [C(3)5(pz)], 104.5 [C4(pz)], 58.5 (CH₂), 57.3 (CH₂), 46.4 [N(CH₃)₂], 30.6 (NCH₃), 12.7 [CH₃(pz)] ppm. IR (Nujol): $\tilde{\nu} = 3206$ (w), 3132 (w), 3086 (w), 1578 (w), 1560 (w), 1508 (m), 1406 (m), 1290 (w), 1107 (w), 1029 (m), 979 (w), 765 (w) cm^{-1} . C₃₈H₇₄Ba₂N₁₄ (1001.79), colorless plates, $0.12 \times 0.10 \times 0.03$ mm, orthorhombic, space group *Cmca* (no. 64), $a = 18.6285(10)$, $b = 15.4487(8)$, $c = 16.6879(9) \text{ \AA}$, $V = 4802.5(4) \text{ \AA}^3$, $Z = 4$, $D_{\text{calcd.}} = 1.39 \text{ g/cm}^3$, $F(000) = 2048$, $T = 90(2) \text{ K}$, $2\theta_{\text{max}} = 60.00^\circ$, 24472 reflections collected, 3597 unique ($R_{\text{int}} = 0.0903$). Final *GooF* = 0.939, $R_1 = 0.0449$, $wR_2 = 0.0817$, R indices based on 3597 reflections with $I > 2\sigma(I)$ (refinement on F^2), 159 parameters, 6 restraints. Lp and absorption corrections applied (ψ scan), $\mu = 1.671 \text{ mm}^{-1}$.

[Ba(Phpz)₂(pmdta)]₂ (2). Method A: A thf solution (50 mL) of Ba{N(SiMe₃)₂}(thf)₂ (0.30 g, 0.50 mmol), phenylpyrazole (1.0 mmol, 0.14 g), and PMDTA (0.10 mL, 0.50 mmol) was refluxed for 12 h. The thf was removed in vacuo and the resulting white precipitate dissolved in toluene. Storage of the solution at -23°C yielded colorless crystals suitable for X-ray studies. Yield: 0.09 g (30%). **Method B:** The general procedure was applied for phenylpyrazole (0.28 g, 2.0 mmol) and PMDTA (0.21 mL,

1.0 mmol). Yield: 0.42 g (70%); m.p. 320°C (dec.) to brown solid; ^1H NMR ($[\text{D}_6]$ benzene): $\delta = 8.18$ [s, 8 H, *o*-H(Ph)], 8.12 [s, 4 H, C5(pz)-H], 7.35 [t, 8 H, *m*-H(Ph)], 7.16 [s, *p*-H(Ph)] (integration not possible due to C₆H₆), 6.95 [s, 4 H, C4(pz)-H], 2.11 (s, 6 H, NCH₃), 1.99 (s, 16 H, CH₂CH₂), 1.70 [s, 24 H, N(CH₃)₂] ppm. ^{13}C NMR ($[\text{D}_6]$ benzene): $\delta = 152.29$ [C3(pz)], 139.8 [C5(pz)], 137.2 [*i*-C(Ph)], 129.1 [*o*-C(Ph)], 126.6 [*m*-, *p*-C(Ph)], 104.5 [C4(pz)], 57.5 (CH₂), 55.7 (CH₂), 45.3 [N(CH₃)₂], 42.6 (NCH₃) ppm. IR (Nujol): $\tilde{\nu} = 2672$ (w), 1601 (s), 1514 (m), 1335 (w), 1286 (m), 1107 (w), 1078 (w), 1053 (m), 1024 (m), 976 (w), 941 (w), 924 (m), 887 (w), 862 (w) cm^{-1} . C₅₄H₇₄Ba₂N₁₄ (1193.9); calcd. C 54.3, H 6.2, Ba 23.0, N 16.4; found C 54.4, H 6.1, Ba 22.6, N 16.1. C₅₄H₇₄Ba₂N₁₄ (1193.95), colorless plates, $0.22 \times 0.22 \times 0.02$ mm, monoclinic, space group *P2₁/c* (no. 14), $a = 12.4638(7)$, $b = 13.1822(8)$, $c = 16.9058(1) \text{ \AA}$, $\beta = 93.9630(1)^\circ$, $V = 2771.0(3) \text{ \AA}^3$, $Z = 2$, $D_{\text{calcd.}} = 1.43 \text{ g/cm}^3$, $F(000) = 1216$, $T = 90(2) \text{ K}$, $2\theta_{\text{max}} = 58.98^\circ$; 13437 reflections collected, 5499 unique ($R_{\text{int}} = 0.0592$). Final *GooF* = 0.805, $R_1 = 0.0396$, $wR_2 = 0.0535$, R indices based on 5499 reflections with $I > 2\sigma(I)$ (refinement on F^2), 316 parameters, 0 restraints. Lp and absorption corrections applied, $\mu = 1.461 \text{ mm}^{-1}$.

[Ba(τ Bupz)₂(pmdta)]₂ (3). Method B: The general procedure was applied for 3-*tert*-butylpyrazole (0.25 g, 2.0 mmol) and PMDTA (0.21 mL, 1.0 mmol). Yield: 0.22 g (40%). **Method C:** Barium (5 mmol, 0.69 g) and 3-*tert*-butylpyrazole (0.29 g, 2.0 mmol) were heated at 200°C in vacuo for 48 h, after which a white powder coated the barium pieces. The white powder was extracted with hexane in which it was slightly soluble. Solubility was increased upon the addition of excess PMDTA. Crystals suitable for X-ray study were formed from this solution after storage at -23°C overnight. Yield: 0.33 g (30%), decomposes over temperature range 70°C (wet) \rightarrow 100 (dry) \rightarrow 170 (wet) \rightarrow 210 (dry) \rightarrow 350 (wet, brown) \rightarrow 374 $^\circ\text{C}$ (melted). ^1H NMR ($[\text{D}_6]$ benzene): $\delta = 7.87$ [s, 4 H, C5(pz)-H], 6.52 [s, 4 H, C4(pz)-H], 2.11 (s, 6 H, NCH₃), 2.08 (b, 16 H, CH₂CH₂N), 1.90 [s, 24 H, N(CH₃)₂], 1.54 [s, 36 H, C(CH₃)₃] ppm. ^{13}C NMR ($[\text{D}_6]$ benzene): $\delta = 162.4$ [C3(pz)], 138.8 [C5(pz)], 104.07 [C4(pz)], 57.8 (CH₂), 56.4 (CH₂), 45.6 [N(CH₃)₂], 42.7 (NCH₃), 32.8 [C(CH₃)₃], 32.5 [C(CH₃)₃] ppm. IR (Nujol): $\tilde{\nu} = 3063$ (w), 1364 (w), 1288 (w), 1204 (w), 1110 (w), 1026 (m), 980 (w), 926 (w), 780 (w), 755 (w), 724 (w) cm^{-1} . C₄₆H₉₀Ba₂N₁₄ (1114.0); calcd. C 49.6, H 8.1, Ba 24.7, N 17.6; found C 49.3, H 8.4, Ba 25.0, N 17.4. C₄₆H₉₀Ba₂N₁₄, (1114.00), colorless plates, $0.26 \times 0.18 \times 0.16$ mm, triclinic, space group *P* $\bar{1}$ (no. 2), $a = 9.8835(5)$, $b = 11.7007(5)$, $c = 12.8989(6) \text{ \AA}$, $\alpha = 72.246(1)$, $\beta = 74.780(1)$, $\gamma = 80.011(1)^\circ$, $V = 1363.71(11) \text{ \AA}^3$, $Z = 1$, $D_{\text{calcd.}} = 1.36 \text{ g/cm}^3$, $F(000) = 576$, $T = 90(2) \text{ K}$, $2\theta_{\text{max}} = 58.00^\circ$; 14998 reflections collected, 7158 unique ($R_{\text{int}} = 0.0308$). Final *GooF* = 1.012, $R_1 = 0.0326$, $wR_2 = 0.0678$, R indices based on 7158 reflections with $I > 2\sigma(I)$ (refinement on F^2), 280 parameters, 0 restraints. Lp and absorption corrections applied, $\mu = 1.478 \text{ mm}^{-1}$.

[Ba(τ Bupz)₂(NH₃)₂]_n (4). Method B: The general procedure was applied for 3-*tert*-butylpyrazole (0.25 g, 2.0 mmol). Colorless needle-like crystals suitable for X-ray studies were obtained overnight at -13°C . Removal of solvent for further characterization resulted in loss of the coordinated ammonia, limiting the characterization of this compound due to reduced solubility. Yield: 0.12 g (30%) for BaN₄C₁₄H₂₂ unit; decomposes over temperature range 135°C (wet) \rightarrow 200 $^\circ\text{C}$ (dry) \rightarrow 261 $^\circ\text{C}$ (melt), suggesting loss of donor. ^1H NMR ($[\text{D}_8]$ thf): $\delta = 7.339$ [s, 2 H, C5(pz)-H], 5.971 [s, 2 H, C4(pz)-H], 1.266 [s, 18 H, C(CH₃)₃] ppm. ^{13}C NMR ($[\text{D}_8]$ thf): $\delta = 160.24$ [C3(pz)], 136.21 [C5(pz)], 101.10 [C4(pz)], 32.74 [C(CH₃)₃], 32.19 [C(CH₃)₃] ppm. IR (Nujol): $\tilde{\nu} = 3348.7$ (s), 2728.9 (w), 1567.0 (m), 1225.2 (w), 1093.1 (s), 1020.2 (s), 929.0 (w), 860.7 (m), 783.2 (m) cm^{-1} . C₁₄H₂₈BaN₆ (417.76), colorless needles,

0.50 × 0.06 × 0.06 mm, triclinic, space group $P\bar{1}$ (no. 2), $a = 8.4996(8)$, $b = 9.7276(9)$, $c = 11.6162(11)$ Å, $\alpha = 89.138(2)$, $\beta = 89.316(2)$, $\gamma = 84.284(2)^\circ$, $V = 955.50(16)$ Å³, $Z = 2$, $D_{\text{calcd.}} = 1.45$ g/cm³, $F(000) = 420$, $T = 90(2)$ K, $2\theta_{\text{max}} = 60.00^\circ$; 10952 reflections collected, 5458 unique ($R_{\text{int}} = 0.0205$). Final $Goof = 1.082$, $R_1 = 0.0299$, $wR_2 = 0.0767$, R indices based on 5458 reflections with $I > 2\sigma(I)$ (refinement on F^2), 209 parameters, 6 restraints. Lp and absorption corrections applied, $\mu = 2.082$ mm⁻¹.

{[Ba(MePhpz)₂(tmeda)]₂} (5). Method B: The general procedure was applied for barium (0.27 g, 2.0 mmol), 3-methyl-5-phenylpyrazole (0.63 g, 4.0 mmol), toluene (40 mL) and TMEDA (1.5 mL) with dry ammonia (10 mL). The solvent was evaporated to 20 mL, and layered with hexane to yield small yellow blocks upon cooling to 0 °C. Yield: 0.68 g (69%); m.p. 135–140 °C. ¹H NMR ([D₆]benzene): $\delta = 8.12$ [s, 8 H, *o*-H(Ph)], 7.36 [t, ³*J*(H,H) = 7.2 Hz, 8 H, *m*-H(Ph)], 7.23 [s, 4 H, *p*-H(Ph)], 6.65 [s, 4 H, C4(pz)-H], 2.36, 2.11 (s, 12 H, Me), 1.78 (s, 32 H, TMEDA) ppm. ¹³C NMR ([D₆]benzene): $\delta = 152.4$ [C(pz)-Ph], 150.3 [C(pz)-Me], 136.1 [*i*-C(Ph)], 129.3 [*o*-C(Ph)], 126.9 [*p*-C(Ph)], 126.1 [*m*-C(Ph)], 105.7 [CH(pz)], 57.6 (NCH₂), 45.3 (CH₃N), 14.1 (Me) ppm. IR (Nujol): $\tilde{\nu} = 3051$ (m), 1949 (w), 1889 (w), 1811 (w), 1762 (w), 1674 (w), 1599 (s), 1568 (s), 1505 (s), 1411 (s), 1292 (m), 1253 (m), 1198 (m), 1161 (m), 1131 (m), 1098 (m), 1071 (m), 1020 (s), 995 (m), 962 (m), 916 (m), 949 (m), 916 (m), 834 (m), 783 (s), 762 (s), 695 (s), 671 (m) cm⁻¹.

{[Ba(Ph₂pz)₂(tmeda)]₂·TMEDA (6). Method B: The general procedure was applied for barium (0.27 g, 2.0 mmol), 3,5-diphenylpyrazole (0.88 g, 4.0 mmol), toluene (10 mL) and TMEDA (15 mL) with condensed anhydrous ammonia (10 mL). Yield: 0.78 g (52%); dec. >350 °C; ¹H NMR ([D₆]benzene): $\delta = 8.03$, [d, ³*J*(H,H) = 8.3 Hz, 16 H, *o*-H(Ph)], 7.36 [t, ³*J*(H,H) = 8.3 Hz, 16 H, *m*-H(Ph)], 7.17 [m, 8 H, *p*-H(Ph)], 7.02 [d, 4 H, C4(pz)-H], 2.22 (s, 12 H, NCH₂), 2.08 (s, 36 H, NCH₃) ppm. ¹³C NMR ([D₆]benzene): $\delta = 129.3$ [*o*-C(Ph)], 126.9 [*p*-C(Ph)], 126.0 [*m*-C(Ph)], 102.2 [C4(pz)], 58.6 (NCH₂), 46.3 (NCH₃) ppm; C(pz)-Ph and *i*-C(Ph) unresolved. IR (Nujol): $\tilde{\nu} = 3059$ (m), 3032 (m), 1946 (w), 1883 (w), 1820 (w), 1751 (w), 1668 (w), 1597 (s), 1522 (m), 1338 (m), 1290 (m), 1260 (m), 1216 (m), 1175 (m), 1155 (m), 1038 (s), 966 (s), 909 (m), 886 (s), 842 (w), 799 (m), 755 (s), 695 (s) cm⁻¹. C₇₈H₉₂Ba₂N₁₄ (1500.29), colorless needles, 0.28 × 0.08 × 0.05 mm, triclinic, space group $P\bar{1}$ (no. 2), $a = 12.821(3)$, $b = 13.055(3)$, $c = 13.758(3)$ Å, $\alpha = 94.26(3)$, $\beta = 110.74(3)$, $\gamma = 111.74(3)^\circ$, $V = 1943.6(11)$ Å³, $Z = 1$, $D_{\text{calcd.}} = 1.183$ g/cm³, $F(000) = 704$, $T = 94(2)$ K, $2\theta_{\text{max}} = 50.00^\circ$; 15865 reflections collected, 6835 unique ($R_{\text{int}} = 0.0326$). Final $Goof = 1.029$, $R_1 = 0.0461$, $wR_2 = 0.1187$, R indices based on 6835 reflections with $I > 2\sigma(I)$ (refinement on F^2), 371 parameters, 108 restraints. Lp and absorption corrections applied, $\mu = 1.050$ mm⁻¹. Heavy disorder of lattice TMEDA could not be handled by refining split positions and required treatment with the “squeeze” function in the PLATON program package.^[21]

[Ba(Ph₂pz)₂(tmeda)]₂·TMEDA (7). Method B: The general procedure was applied for barium (0.27 g, 2.0 mmol), 3,5-diphenylpyrazole (0.88 g, 4.0 mmol), toluene (20 mL) and TMEDA (30 mL), with condensed anhydrous ammonia (10 mL). The solvent was reduced to 20 mL and cooling to -20 °C yielded colorless prisms. Yield: 0.47 g (51%); m.p. >350 °C; ¹H NMR ([D₆]benzene): $\delta = 8.10$ [d, ³*J*(H,H) = 7.5 Hz, 8 H, *o*-H(Ph)], 7.41 [t, ³*J*(H,H) = 7.6 Hz, 8 H, *m*-H(Ph)], 7.32 [s, 2 H, C4(pz)-H], 7.21 [t, ³*J*(H,H) = 7.3 Hz, 4 H, *p*-H(Ph)], 2.14, 1.98 (br. d, 32 H, TMEDA) ppm, indicating loss of the lattice TMEDA molecule. ¹³C NMR ([D₆]benzene): $\delta = 152.2$ [C(pz)-Ph], 136.6 [*ipso*-C(Ph)], 129.6 [*o*-C(Ph)], 126.7 [*p*-C(Ph)], 125.9 [*m*-C(Ph)], 103.1 [C4(pz)], 58.1 (NCH₂), 46.1 (NCH₃) ppm. IR (Nujol): $\tilde{\nu} = 3062$ (m), 3031 (m), 1945 (w), 1874 (w), 1800

(w), 1743 (w), 1665 (w), 1601 (s), 1526 (m), 1511 (m), 1359 (m), 1337 (m), 1292 (m), 1264 (m), 1218 (m), 1180 (w), 1161 (m), 1133 (m), 1098 (w), 1076 (m), 1052 (s), 1031 (s), 965 (s), 945 (m), 909 (m), 836 (m), 808 (m), 784 (s), 756 (s), 730 (w), 695 (s) cm⁻¹. C₄₈H₇₀BaN₁₀ (924.46), colorless blocks, 0.30 × 0.22 × 0.18 mm, monoclinic, space group $C2/c$, $a = 26.023(2)$, $b = 11.970(1)$, $c = 17.170(1)$ Å, $\beta = 114.084(1)^\circ$, $V = 4882.67$ Å³, $Z = 4$, $D_{\text{calcd.}} = 1.100$ g/cm³, $F(000) = 1672$, $T = 123(2)$ K, $2\theta_{\text{max}} = 55.00^\circ$; 23882 reflections collected, 5609 unique ($R_{\text{int}} = 0.0281$). Final $Goof = 1.117$, $R_1 = 0.0251$, $wR_2 = 0.0645$, R indices based on 5609 reflections with $I > 2\sigma(I)$ (refinement on F^2), 294 parameters, 84 restraints. Lp and absorption corrections applied, $\mu = 0.846$ mm⁻¹. Compound 7 contains a lattice TMEDA molecule, which was highly disordered, non-resolvable, and therefore removed from the crystal structure refinement using the “squeeze” function in the program package PLATON.^[21]

Supporting Information (see footnote on the first page of this article): Additional structure descriptions, selected bond lengths and angles for compounds 1–4, 6, and 7.

Acknowledgments

We gratefully acknowledge support from the National Science Foundation (CHE-0108098 and CHE-0505863), and the Australian Research Council. Purchase of the X-ray diffraction equipment was made possible with grants from the National Science Foundation (CHE-9527858 and CHE-0234912), Syracuse University and the W. M. Keck Foundation.

- [1] L. G. Hubert-Pfalzgraf, *J. Mater. Chem.* **2004**, *14*, 3113–3123.
- [2] G. A. Battiston, R. Gerbasi, G. Carta, F. Marchetti, C. Pettinari, A. Rodriguez, D. Barreca, C. Maragno, E. Tondello, *J. Electrochem. Soc.* **2006**, *153*, F35–F38.
- [3] a) H. M. El-Kaderi, M. J. Heeg, C. H. Winter, *Polyhedron* **2005**, *24*, 645–653; b) H. M. El-Kaderi, M. J. Heeg, C. H. Winter, *Eur. J. Inorg. Chem.* **2005**, 2081–2088.
- [4] a) J. Hitzbleck, G. B. Deacon, K. Ruhlandt-Senge, *Eur. J. Inorg. Chem.* **2007**, 592–601; b) J. Hitzbleck, A. Y. O'Brien, G. B. Deacon, K. Ruhlandt-Senge, *Inorg. Chem.* **2006**, *45*, 10329–10337; c) J. Hitzbleck, G. B. Deacon, K. Ruhlandt-Senge, *Angew. Chem. Int. Ed.* **2004**, *43*, 5218–5220; d) J. Hitzbleck, A. Y. O'Brien, C. M. Forsyth, G. B. Deacon, K. Ruhlandt-Senge, *Chem. Eur. J.* **2004**, *10*, 3315–3323.
- [5] I. Kobrsi, J. E. Knox, M. J. Heeg, H. B. Schlegel, C. H. Winter, *Inorg. Chem.* **2005**, *44*, 4894–4896.
- [6] D. Pfeiffer, M. J. Heeg, C. H. Winter, *Inorg. Chem.* **2000**, *39*, 2377–2384.
- [7] a) A. F. Wells, *Structural Inorganic Chemistry*, 5th ed., Oxford, Clarendon, **1984**; b) L. Pauling, *The Nature of the Chemical Bond*, 3rd ed., Cornell University Press, Ithaca, NY, **1960**.
- [8] a) A. Y. O'Brien, Doctoral Thesis, Syracuse University, Syracuse, NY, **2005**; b) J. Hitzbleck, Doctoral Thesis, Syracuse University, Syracuse, NY, **2004**.
- [9] A. Steiner, G. T. Lawson, B. Walford, D. Leusser, D. Stalke, *J. Chem. Soc. Dalton Trans.* **2001**, 219–221.
- [10] a) G. B. Deacon, C. M. Forsyth, A. Gitlits, R. Harika, P. C. Junk, B. W. Skelton, A. H. White, *Angew. Chem. Int. Ed.* **2002**, *41*, 3249–3251; b) S. Beaini, G. B. Deacon, A. P. Erven, P. C. Junk, D. R. Turner, *Chem. Asian J.* **2007**, *2*, 539–550; c) S.-Á. Cortés-Llamas, R. Hernández-Lamonedá, M.-Á. Velázquez-Carmona, M.-A. Muñoz-Hernández, R. A. Toscano, *Inorg. Chem.* **2006**, *45*, 286–294; d) G. B. Deacon, B. M. Gatehouse, S. Nickel, S. N. Platts, *Aust. J. Chem.* **1991**, *44*, 613–621; e) J. E. Cosgriff, G. B. Deacon, B. M. Gatehouse, H. Hemling, H. Schumann, *Angew. Chem. Int. Ed. Engl.* **1993**, *32*, 871–875; f) J. E. Cosgriff, G. B. Deacon, B. M. Gatehouse, *Aust. J. Chem.*

- 1993, 46, 1881–1896; g) J. E. Cosgriff, G. B. Deacon, B. M. Gatehouse, H. Hemling, H. Schumann, *Aust. J. Chem.* **1994**, 47, 1223–1235; h) J. E. Cosgriff, G. B. Deacon, B. M. Gatehouse, P. R. Lee, H. Schumann, *Z. Anorg. Allg. Chem.* **1996**, 622, 1399–1403; i) J. E. Cosgriff, G. B. Deacon, G. D. Fallon, B. M. Gatehouse, H. Schumann, R. Weiman, *Chem. Ber.* **1996**, 129, 953–958; j) J. E. Cosgriff, G. B. Deacon, *Angew. Chem. Int. Ed.* **1998**, 37, 286–287; k) G. B. Deacon, E. E. Delbridge, B. W. Skelton, A. H. White, *Eur. J. Inorg. Chem.* **1998**, 543–545; l) G. B. Deacon, E. E. Delbridge, B. W. Skelton, A. H. White, *Angew. Chem. Int. Ed.* **1998**, 37, 2251–2252; m) J. E. Cosgriff, G. B. Deacon, E. E. Delbridge, C. Jones, B. W. Skelton, A. H. White, *Mater. Sci. Forum* **1999**, 315–317, 136–143; n) G. B. Deacon, E. E. Delbridge, B. W. Skelton, A. H. White, *Eur. J. Inorg. Chem.* **1999**, 751–761; o) G. B. Deacon, E. E. Delbridge, C. M. Forsyth, *Angew. Chem. Int. Ed.* **1999**, 38, 1766–1767; p) G. B. Deacon, A. Gitlis, B. W. Skelton, A. H. White, *Chem. Commun.* **1999**, 1213–1214; q) G. B. Deacon, E. E. Delbridge, C. M. Forsyth, P. C. Junk, B. W. Skelton, A. H. White, *Aust. J. Chem.* **1999**, 52, 733–739; r) G. B. Deacon, E. E. Delbridge, C. M. Forsyth, B. W. Skelton, A. H. White, *J. Chem. Soc. Dalton Trans.* **2000**, 745–751; s) G. B. Deacon, E. E. Delbridge, G. D. Fallon, C. Jones, D. E. Hibbs, M. B. Hursthouse, B. W. Skelton, A. H. White, *Organometallics* **2000**, 19, 1713–1721; t) G. B. Deacon, A. Gitlits, P. W. Roesky, M. K. Burgstein, K. C. Lim, B. W. Skelton, A. H. White, *Chem. Eur. J.* **2001**, 7, 127–138; u) G. B. Deacon, E. E. Delbridge, D. J. Evans, R. Harika, P. C. Junk, B. W. Skelton, A. H. White, *Chem. Eur. J.* **2004**, 10, 1193–1204; v) G. B. Deacon, C. M. Forsyth, A. Gitlits, B. W. Skelton, A. H. White, *Dalton Trans.* **2004**, 1239–1247; w) S. Beaini, G. B. Deacon, M. Hilder, P. C. Junk, D. R. Turner, *Eur. J. Inorg. Chem.* **2006**, 3434–3441.
- [11] N. C. Mösch-Zanetti, M. Ferbinteanu, J. Magull, *Eur. J. Inorg. Chem.* **2002**, 950–956.
- [12] a) A. R. Katritzky, I. Ghiviriga, P. J. Steel, D. C. Oniciu, *J. Chem. Soc. Perkin Trans. 2* **1996**, 443; b) P. Fischer, A. Fettig, *Magn. Reson. Chem.* **1997**, 35, 839; c) B. K. Shull, D. E. Spielvogel, R. Gopaldaswamy, S. Sankar, P. D. Boyle, G. Head, K. Devito, *J. Chem. Soc. Perkin Trans. 2* **2000**, 557; d) H. S. Gutowsky, C. H. Holm, *J. Chem. Phys.* **1956**, 25, 1228; e) J. B. Lambert, L. Lin, *Magn. Reson. Chem.* **2001**, 39, 714; f) Sandström, *J. Dynamic NMR Spectroscopy*, Academic Press, New York, **1982**, p. 93.
- [13] M. Westerhausen, *Inorg. Chem.* **1991**, 30, 96.
- [14] S. Trofimenko, J. C. Calabrese, J. S. Thompson, *Inorg. Chem.* **1987**, 26, 1507–1514.
- [15] J. Elguero, E. Gonzalez, R. Jacquier, *Bull. Soc. Chim. Fr.* **1968**, 707–713.
- [16] M. Westerhausen, *Trends Organomet. Chem.* **1997**, 2, 89–105.
- [17] J. Elguero, E. Gonzalez, R. Jacquier, *Bull. Soc. Chim. Fr.* **1966**, 2832.
- [18] H. Hope, *Prog. Inorg. Chem.* **1994**, 41, 1.
- [19] G. M. Sheldrick, University of Göttingen, Göttingen, Germany, **1996**.
- [20] G. M. Sheldrick, Siemens, Madison, WI, USA, **1999**.
- [21] a) A. L. Spek, *Acta Crystallogr., Sect. A* **1990**, 46, C34; b) *PLATON – A Multipurpose Crystallographic Tool*, Utrecht University, Utrecht, The Netherlands, **2005**.

Received: September 20, 2007

Published Online: November 15, 2007